A proposed damage gradient model for the sequential disordering induced in Sc-Ni multilayers by ion irradiation

2002 J. Phys.: Condens. Matter 14 731

(http://iopscience.iop.org/0953-8984/14/4/308)

INSTITUTE OF PHYSICS PUBLISHING JOURNAL OF PHYSICS: CONDENSED MATTER

J. Phys.: Condens. Matter **14** (2002) 731–737 PII: S0953-8984(02)27959-X

A proposed damage gradient model for the sequential disordering induced in Sc–Ni multilayers by ion irradiation

L Hu, Z F Li, W S Lai and B X Liu[1]

Advanced Materials Laboratory, Department of Material Science and Engineering, Tsinghua University, Beijing 100084, People's Republic of China

E-mail: dmslbx@tsinghua.edu.cn

Received 16 August 2001, in final form 5 November 2001
Published 18 January 2002
Online at stacks.iop.org/JPhysCM/14/731

Abstract

An abnormal sequential disordering process was observed in Sc–Ni multilayers upon room temperature 200 keV xenon-ion irradiation: the Ni lattice became unstable and entered an amorphous state faster than the Sc lattice did. Since there was negligible difference in mutual solid solubility and no significant difference in melting point between the two metals, this abnormal process was attributed to the fact that the damage density in the Ni layer was calculated to be about 2–3 times that in the Sc. A damage gradient model was thus proposed in which the Sc atoms diffused much faster along an uphill damage gradient towards the Ni layer than vice versa, resulting in the Ni lattice exceeding its critical solid solubility and collapsing into a disordered state faster than the Sc lattice.

1. Introduction

Since the early 1980s, ion beam mixing (IBM) of metal–metal multilayers has been used to produce non-equilibrium alloys in binary metal systems [1]. Already, a great number of amorphous and other metastable alloys have been obtained in numerous systems with different characteristics [2]. Meanwhile, a great effort has been made to investigate the detailed mechanism involved in the amorphization process consequent upon IBM; e.g. Ding *et al* [3] have observed the dependence of temperature upon the ion and electron irradiation, Averback and Ghaly [4] conducted molecular dynamics (MD) simulations to study the effect of ions impinging on condensed matter and Krill *et al* [5] studied the effect of supersaturated solid solubility on amorphization behaviour under the guidance of the Lindemann melting criterion. Generally speaking, a clear physical picture describing the detailed process of the irradiation-induced amorphization transition has not been developed, because of the complexity involved

[1] Author to whom any correspondence should be addressed.

in the IBM far-from-equilibrium process. Also, in the early 1980s, an amorphization transition in metal–metal multilayers was observed upon solid-state reaction (SSR) being conducted at a medium temperature, i.e. the crystalline Au and La transformed into an amorphous phase upon thermal annealing at about 350 °C [6]. In SSR studies, an 'asymmetric amorphization behaviour' was observed during SSR in some binary metal systems in experiments and/or by means of MD simulations, i.e. the growth of the amorphous interlayer towards one metal is faster than towards the other. In some cases, the amorphous interlayer grew faster towards the metal with the lower melting point [7–11]. Recently, however, an opposite growth behaviour was reported by Lai and Liu [12] in the Ni–Ti system: the speed growth of the amorphous interlayer was faster towards Ti with a melting point of 1941 K than towards Ni, whose melting point (1728 K) is lower than that of Ti. From a physical point of view, the origin of the amorphization transition was the initial crystalline lattice collapsing into a disordered state while the solute concentration exceeded the critical solid solubility allowed by the lattice, with the other possible influencing factors, e.g. strain and grain size, playing a secondary role. On the basis of this understanding, Lai and Liu [13] proposed a solubility criterion, which predicted that the amorphous interlayer would grow faster during SSR towards the metal with the lower critical solid solubility. It turned out that the prediction was in good agreement with the experimental observations and/or MD simulation results reported so far in the literature.

To test whether the solubility criterion was also valid for the process of the irradiation-induced amorphization transition in metal–metal multilayers, Li and Liu [14] investigated the Ni–W system—in which the solid solubility of Ni in W is much lower than that of W in Ni—and did observe that the W-enriched multilayers were easier to amorphize upon ion irradiation than the Ni-enriched ones, though the metal W has a much higher melting point than Ni. Apparently, such asymmetry of behaviour induced in the Ni–W multilayers by ion irradiation could be attributed to a solid-solubility difference between the two metals. In the present study, the Sc–Ni system was chosen to use to investigate whether or not asymmetric amorphization behaviour would also emerge in Sc–Ni multilayers upon ion irradiation and, if so, what would be the predominant governing factor, as the solid solubilities of Sc in Ni and Ni in Sc are almost identical, both being less than 1%. In addition, the Sc–Ni system is characterized by a very negative formation enthalpy (-57 kJ mol^{-1}) and there is no significant difference in melting point between Sc (1812 K) and Ni (1726 K) [15].

2. Experimental procedure

The Sc–Ni multilayers were prepared by alternate depositions of pure Sc and Ni onto freshly cleaved NaCl single crystals in an electron-gun evaporation system with a vacuum level of the order of 10^{-8} Torr. The deposition rate was controlled at 0.5 Å s^{-1} and no special cooling were provided for the substrates during deposition. The total thickness of the films was designed to be about 40 nm. Three alloy compositions, i.e., $Sc_{80}Ni_{20}$, $Sc_{50}Ni_{50}$ and $Sc_{30}Ni_{70}$, were chosen for the present study. The Sc–Ni multilayered samples were designed to consist of six Sc and six Ni layers and the desired overall compositions were obtained by adjusting the relative thicknesses of the individual Sc and Ni layers. The real compositions of the samples were confirmed to be $Sc_{80}Ni_{20}$, $Sc_{52}Ni_{48}$ and $Sc_{29}Ni_{71}$, respectively, by energy-dispersive spectrum (EDS) analysis with a measuring error around 4%. 200 keV xenon ions were employed for the ion irradiation experiments and the irradiating xenon ions were able to penetrate through the Sc–Ni multilayers of about 40 nm thickness with a good mixing efficiency. The IBM experiments were conducted at 77 K, i.e. the sample holders were always cooled by liquid nitrogen during the ion irradiation, to various doses ranging from 1×10^{14} to 6×10^{15} Xe^+ cm^{-2}. The vacuum level of the implanter was of the order of 10^{-6} Torr. The xenon-ion current density

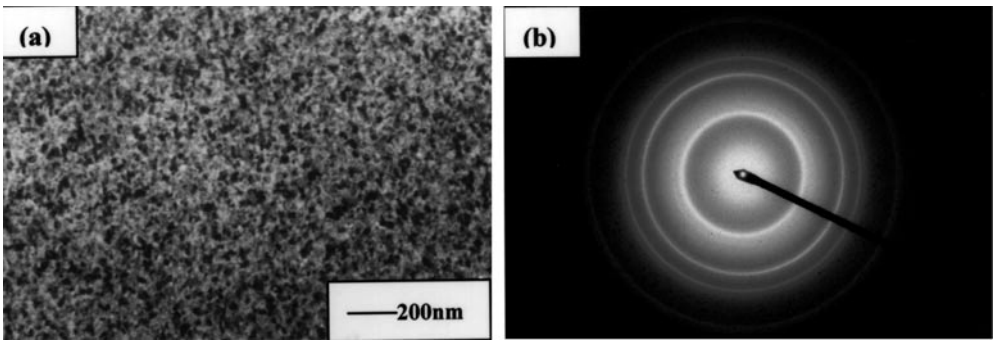

Figure 1. (a) A bright-field image of the as-deposited $Sc_{80}Ni_{20}$ multilayered films. (b) A corresponding SAD pattern, showing the diffraction lines of the polycrystalline Sc and the polycrystalline Ni together with a weak halo reflected from the Sc–Ni amorphous phase.

was limited to about 0.5 μA cm^{-2} to avoid an otherwise possible overheating effect. With such precautions, the temperature rise of the substrates during the ion irradiation was estimated to be around 150 °C. In other words, the real temperature of the substrates during ion irradiation was still lower than room temperature, and so would have no very considerable effect on the non-equilibrium phase formation [2]. For structural characterization, all the Sc–Ni multilayered films were removed from the NaCl substrates with de-ionized water and placed onto the Cu grids for transmission electron microscopy (TEM) examination and selected-area diffraction (SAD) analysis.

3. Results

We now present the experimental results. Firstly, the structures that emerged in the as-deposited multilayered films with the three different overall compositions were basically the same. Take the $Sc_{80}Ni_{20}$ multilayered sample as an example; figures 1(a) and (b) show a bright-field image and the corresponding SAD pattern obtained for the as-deposited $Sc_{80}Ni_{20}$ multilayers. One can see, in figure 1(b), the sharp and intense diffraction lines from Sc and Ni, confirming the presence of polycrystalline Sc and Ni in the as-deposited state. Carefully examination of the SAD pattern reveals that there is one halo of weak intensity located somewhere in the midst of the strongest Sc(100) and Ni(111) lines, suggesting that a trace of Sc–Ni amorphous phase has already been formed during deposition—most probably in the Sc–Ni interfacial regions.

Table 1 lists the structural changes that emerged in the Sc–Ni multilayers upon 200 keV xenon-ion irradiation to various doses. One can observe from the table that a single amorphous phase was formed in all of the Sc–Ni multilayered films with the three different overall compositions, yet the doses required to induce complete amorphization were different, i.e. they were 9×10^{14}, 4×10^{15} and 4×10^{15} Xe^+ cm^{-2} for the $Sc_{30}Ni_{70}$, $Sc_{50}Ni_{50}$ and $Sc_{80}Ni_{20}$ multilayers, respectively. These results suggested that in the Sc–Ni system with a large negative formation enthalpy, amorphous alloy films were readily obtained by the IBM scheme over a relatively abroad composition range.

More interestingly, one can also observe from the table that some intermediate states emerged in the Sc–Ni multilayered films during the early stages of the IBM before the single Sc–Ni amorphous phase formed. Take the $Sc_{52}Ni_{48}$ multilayered sample as an example. Figure 2(a) and (b) are two SAD patterns for the $Sc_{52}Ni_{48}$ multilayered films, presented to show the structural evolution after irradiation to doses of 3×10^{14} and 4×10^{15} Xe^+ cm^{-2},

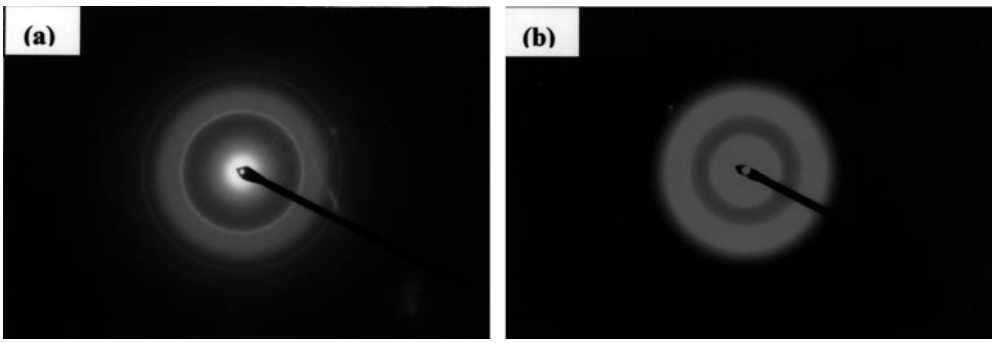

Figure 2. (a) An SAD pattern taken from the $Sc_{52}Ni_{48}$ multilayered films after 200 keV xenon IBM at 77 K to a dose of 3×10^{14} Xe^+ cm^{-2}. One can see one halo from the amorphous Sc–Ni phase formed and some weak diffraction lines from polycrystalline Sc, meaning that at this irradiation stage, a trace of Sc remained in the crystalline structure. (b) A SAD pattern taken at an irradiation dose of 4×10^{15} Xe^+ cm^{-2}. One can see only diffraction halos, confirming the formation of a single amorphous Sc–Ni phase in the sample.

Table 1. The structural phase transformation that emerged in the Sc–Ni multilayered films during 200 keV xenon-ion irradiation at 77 K to various doses ranging from 1×10^{14} to 4×10^{15} Xe^+ cm^{-2}.

Dose (Xe^+ cm^{-2})	$Sc_{29}Ni_{71}$	$Sc_{52}Ni_{48}$	$Sc_{80}Ni_{20}$
1×10^{14}	Sc + Ni	Sc + Ni	Sc + Ni
3×10^{14}	Sc + amorphous	Sc + amorphous	Sc + amorphous
5×10^{14}	Sc + amorphous	Sc + amorphous	Sc + amorphous
7×10^{14}	Sc + amorphous	Sc + amorphous	Sc + amorphous
9×10^{14}	Amorphous	Sc + amorphous	Sc + amorphous
2×10^{15}	Amorphous	Sc + amorphous	Sc + amorphous
4×10^{15}	Amorphous	Amorphous	Amorphous

respectively. In figure 2(a), one observes one halo together with some very weak diffraction lines from Sc, meaning that in this intermediate state, the Ni lattice has already become disordered in forming the observed Sc–Ni amorphous phase, while a trace amount of Sc still remained in the crystalline structure. The above phenomenon clearly revealed that a sequential disordering or asymmetric amorphization behaviour did take place in the Sc–Ni multilayers upon ion irradiation. It was further clarified later that the asymmetric amorphization behaviour originated from it being easier to disorder the Ni lattice than the Sc lattice under the present experimental conditions. From figure 2(b), one observes three halos, but no diffraction line remains, indicating that a single Sc–Ni amorphous phase was formed at an irradiation dose of 4×10^{15} Xe^+ cm^{-2}. In summary, the above structural evolution that emerged in the $Sc_{52}Ni_{48}$ multilayered sample can be expressed as follows:

$$\text{Sc + Ni} \xrightarrow{3\times10^{14}\ \text{Xe}^+\ \text{cm}^{-2}} \text{amorphous + Sc (trace)} \xrightarrow{4\times10^{15}\ \text{Xe}^+\ \text{cm}^{-2}} \text{amorphous.}$$

Similar phenomena were also observed for the other two compositions, as shown in table 1.

4. Discussion

It is well known that IBM is a far-from-equilibrium process and very capable of producing non-equilibrium alloys. The formation of uniform Sc–Ni amorphous alloys upon IBM could

be explained by a well-established two-step mechanism involved in the process, i.e. atomic collision cascade and relaxation [2]. Briefly, the atomic collision cascade induces intermixing between the Sc and Ni layers, resulting in a highly energetic and disordered Sc–Ni mixture, while the relaxation with a very short time span (10^{-10}–10^{-9} s) prevents the possible crystalline phase from growing [16], thus leading to the formation of the Sc–Ni amorphous alloy phase. The main issue here is therefore the underlying physics responsible for the asymmetric amorphization behaviour or sequential disordering observed in the Sc–Ni system.

As mentioned in the introduction, a metal lattice becomes unstable and enters an amorphous state mainly because the solute concentration exceeds its maximum solid solubility, as has been confirmed by experimental observations and by means of MD simulations in some binary metal systems [12, 13, 17]. In the present case of the Sc–Ni system, the experimental observations showed that the Ni lattice became disordered faster than the Sc lattice, indicating that the Ni lattice reached and exceeded its critical solid solubility faster than the Sc lattice. Nonetheless, there was essentially no difference between the critical solid solubilities of Sc in Ni and Ni in Sc. It was therefore deduced that the Sc atoms diffused into the Ni layer with a greater speed than the Ni atoms diffused into the Sc layer if the thicknesses of the Ni and Sc layers were about the same. It should be noted, however, that for the $Sc_{52}Ni_{48}$ multilayered sample, the thickness of the individual Sc layer was nearly 2.5 times that of the Ni layer, i.e. the diffusion lengths for Sc and Ni atoms migrating into the partner lattices were different, which made it complicated to clarify the underlying physics for the observed asymmetric behaviour.

To exclude the influence of the difference in layer thickness, we investigated another case of a $Sc_{29}Ni_{71}$ multilayered sample in which the thicknesses of the individual Sc and Ni layers were approximately the same, corresponding to similar diffusion lengths for the Sc and Ni atoms diffusing into their partners. Similar IBM experiments were performed and the same intermediate state was observed in the $Sc_{29}Ni_{71}$ multilayered sample—i.e. after irradiation to a dose of 3×10^{14} Xe^+ cm^{-2}, the corresponding SAD pattern showed one halo together with some very weak diffraction lines from Sc, meaning that in this intermediate state, the Ni lattice has already become disordered in forming the observed Sc–Ni amorphous phase, while a trace amount of Sc still remained in the crystalline structure, confirming again an easier disordering of the Ni lattice than the Sc lattice in the $Sc_{29}Ni_{71}$ multilayered sample. On the basis of the understanding that a crystalline lattice would collapse when the solute concentration exceeds its critical value, it was deduced that the Sc atoms should have diffused faster into the Ni lattice than the Ni atoms into the Sc lattice in the $Sc_{29}Ni_{71}$ multilayered sample, since the thicknesses of the Sc and Ni layers as well as the critical solid solubilities of Sc in Ni and Ni in Sc were approximately the same.

It was thought that in the Sc–Ni multilayers, the atomic collision triggered by ion irradiation would induce intermixing between the Sc and Ni metal layers, as a great number of Sc and Ni atoms were excited by the impinging xenon ions into motion and so migrate, crossing the interfaces, thus resulting in Sc dissolving into Ni and Ni into Sc. In our case, the sample was in an arrangement of Sc–Ni multilayers and the initial energy of the irradiating xenon ions was of 200 keV. When the irradiating xenon ions penetrated the sample, the energy of the irradiating ions varied due to the energy loss in the sample. Employing the TRIM program [18], it was calculated that the energy of the xenon ions was reduced gradually and eventually reached a value of about 9 keV at the end of the Sc–Ni multilayered sample. For the approximation, the Sc–Ni multilayers were divided into twelve single layers (or six bilayers) and the ratio of the vacancies to ions in each single layer was calculated using the respective energy values according to the energy-loss calculation. Take the third Sc–Ni bilayer as an example; using the energy of irradiating xenon ions of 100 keV, the ratio of the vacancies to ions in the Ni layer

was calculated to be 284.3, which was more than three times that in the Sc layer, calculated to be 91.6, indicating that there existed a sharp radiation damage gradient across the Sc–Ni interface. Similar calculations were also performed for the other five bilayers. It turned out that although the numbers of vacancies and ions in individual Ni and Sc layers changed slightly, the damage gradient across the Sc–Ni interfaces basically remained the same, i.e. the damage ratio in the Ni layers was more than three times that in the Sc layers. In other words, the number of vacancies created in the Ni layers was considerably higher than the number created in the Sc layers. It is known that the radiation damage would help in inducing disordering in the materials and that the heavier the damage, the more readily the materials become disordered. In the present case, the damage in the Ni layers was heavier than that in the Sc layers, which could therefore help in producing a faster disordering of Ni lattice than in the Sc lattice. Nonetheless, for the Ni lattice transforming into an amorphous state, the dissolving of Sc atoms should also be considered; this is discussed further in the next paragraph.

On the basis of the above experimental results, we proposed the following mechanism: in the $Sc_{29}Ni_{71}$ multilayers, so sharp a damage gradient across the Sc–Ni interfaces could drive a differential interdiffusion, i.e. the Sc atoms could migrate faster into the vacancy sites in the Ni layers than in the Sc layers, because the vacancy density in the Ni layers was much higher than that in the Sc layers. In the interdiffusion process, the moving Sc and Ni atoms could be either lattice atoms (jumping into vacancies) or interstitials (jumping into vacancies). Since the solid solubilities at the Ni end and the Sc end were quite similar, the solute concentration of the Sc atoms in the Ni lattice could therefore exceed the critical solid solubility faster than that of the Sc atoms in the Ni lattice, which in turn resulted in an asymmetric growth of the Sc–Ni amorphous phase. The proposed interpretation was apparently in good agreement with the experimental observations mentioned above. Incidentally, the concept of radiation damage gradient has also been employed in explaining the interfacial reaction between deposited metal layers on silicon substrates [19].

One may suggest another mode of mutual diffusion as follows. Since there were more Ni interstitials than Sc, more Ni atoms would diffuse into and reside in the interstitial sites in the Sc layers. If such a mechanism were operative, the Sc lattice would have become disordered faster than the Ni lattice, which is not compatible with the experimental observations. Another alternative is that both Ni and Sc interstitial atoms jump into the vacancy sites of the Sc and Ni layers, respectively, and therefore the jumping speed should be in positive proportion to the numbers of vacancy sites available in the Sc and Ni layers for the Ni and Sc atoms to reside in, respectively. Since the vacancy density in the Ni layers was more than three times that in the Sc layers, the diffusion speed of Sc atoms into Ni layers would be faster than that of Ni atoms into Sc layers. This interstitial–vacancy jumping mechanism has already been included in the above model proposed by the present authors.

Also, for another two Sc–Ni multilayers, the individual Sc layers were thicker (because of the higher Sc contents) than that in the $Sc_{29}Ni_{71}$ sample. From the above damage gradient model, it was deduced that the irradiation doses required to effect complete amorphization in these samples should be higher than that for the $Sc_{29}Ni_{71}$ multilayered sample and this deduction was in excellent agreement with the experimental results listed in table 1.

Incidentally, in the defect creation upon ion irradiation, there were equal numbers of interstitials and vacancies in Sc and Ni layers. It is known that during the defect creation process, some of the interstitials could be combined with vacancies, resulting in a reduction of the existing numbers of interstitials and vacancies in both Sc and Ni layers. Nonetheless, a sharp damage gradient across the Sc and Ni interfaces could still be created and not eliminated by such a recombination process. As long as there was a sharp damage gradient, it could drive

a differential diffusion and result in an asymmetric growth of the Sc–Ni amorphous phase as observed in the IBM experiments.

5. Summary

In conclusion, we have shown that in the Sc–Ni system, in which the maximum solid solubilities at both extremes were essentially identical, a sharp damage gradient created across the Sc–Ni interfaces by ion irradiation played a predominant role in governing the asymmetric amorphization behaviour, i.e. under similar irradiation conditions, the metal subjected to higher damage density would collapse faster than its less damaged partner metal, because the more highly damaged metal would reach its critical solid solubility faster by dissolving the solute atoms than the less damaged metal.

Acknowledgments

The financial aid for this study from the National Natural Science Foundation and the Ministry of Science and Technology (grant No G2000067207) of China is gratefully acknowledged. Our thanks also go to Mr Z C Li and Mr X Q Cheng in this group and to the staff at Electron Microscopy Laboratory of Peking University for their kind help.

References

[1] Liu B X, Johnson W L, Nicolet M-A and Lau S S 1983 *Appl. Phys. Lett.* **42** 45
[2] Liu B X, Lai W S and Zhang Q 2000 *Mater. Sci. Eng.: Rep.* **29** 1–48
[3] Ding F R, Okamoto P R and Rehn L E 1989 *J. Mater. Res.* **4** 1444
[4] Averback R S and Ghaly M 1997 *Nucl. Instrum. Methods* B **127** 709
[5] Krill C E III, Li J, Garland C M, Ettl C, Samwer K, Yelon W B and Johnson W L 1995 *J. Mater. Res.* **10** 280
[6] Schwarz R B and Johnson W L 1983 *Phys. Rev. Lett.* **51** 415
[7] Yang G W, Lin C and Liu B X 1999 *J. Mater. Res.* **14** 3027
[8] Lai W S and Liu B X 1998 *Phys. Rev.* B **58** 6063
[9] Zhang Q, Lai W S and Liu B X 2000 *Phys. Rev.* B **61** 9345
[10] Zhang Q, Lai W S and Liu B X 2000 *Eur. Phys. J.* B **16** 223
[11] Zhang Q, Lai W S and Liu B X 1998 *Phys. Rev.* B **58** 14 020
[12] Lai W S and Liu B X 2000 *J. Phys. Soc. Japan* **9** 2923
[13] Lai W S and Liu B X 2001 *Phil. Mag. Lett.* **81** 45
[14] Li Z F and Liu B X 2001 *Japan. J. Appl. Phys.* submitted
[15] de Boer F R, Boom R, Mattens W C M, Miedema A R and Niessen A K 1989 *Cohesion in Metals: Transition Metal Alloys* (Amsterdam: North-Holland)
[16] Thompson M W 1969 *Defects and Radiation Damage in Metals* (Cambridge: Cambridge University Press) chs 4–5
[17] Zhang Q, Lai W S and Liu B X 1999 *Phys. Rev.* B **59** 13 521
[18] Biersack J P and Ziegler J F 1985 *The Stopping and Range of Ions in Solids* (New York: Pergamon)
[19] Tao K, Hewett C A and Lau S S 1987 *Nucl. Instrum. Methods Phys. Res.* B **19/20** 753